Euro. Jnl of Applied Mathematics (2006), *vol.* 17, *pp.* 435–463.
doi:10.1017/S0956792506006620 First published online 21 August 2006 Printed in the United Kingdom

Bistable nematic liquid crystal device with flexoelectric switching

L. J. CUMMINGS and G. RICHARDSON

School of Mathematical Sciences, University of Nottingham, Nottingham NG7 2RD, UK

(*Received 12 December 2005; revised 15 May 2006*)

Motivated generally by potential applications in the liquid crystal display industry [8,35], and specifically by recent experimental, theoretical and numerical work [6,7,13,14,21,25,30,31], we consider a thin film of nematic liquid crystal (NLC), sandwiched between two parallel plates. Under certain simplifying assumptions, laid out in §2, we find that for monostable surfaces (i.e. only a single preferred director anchoring angle at each surface), two optically-distinct, steady, stable (equal energy) configurations of the director are achievable, that is, a bistable device. Moreover, it is found that the stability of both of these steady states may be destroyed by the application of a sufficiently large electric field, and that switching between the two states is possible, via the flexoelectric effect. Such a phenomenon could be used in NLC display devices, to reduce power consumption drastically. Previous theoretical demonstrations of such (switchable) bistable devices have either relied on having bistable bounding surfaces, that is, surfaces at which there are *two* preferred director orientations at the surface [7,14]; on having special (nonplanar) surface morphology within the cell that allows for two stable states (the zenithal bistable device (ZBD) [4,21]; or, in the case of the Nemoptic BiNem technology [11,19], on flow effects and a very carefully applied electric field to effect the switching.

1 Introduction

In this paper we use a simple model to describe the steady states of a thin film of nematic liquid crystal (NLC) bounded by rigid walls, and investigate how an electric field may be used to switch between steady states. The original motivation for our study was work carried out at Hewlett-Packard laboratories in Bristol, where switchable bistable nematic devices operating via the flexoelectric effect have been made experimentally, and reproduced in numerical calculations that are reported in Newton & Spiller [21].

NLC display devices rely on the fact that the optical properties of a NLC depend on the alignment of its molecules, which are typically long and thin ('rod-like'). The equilibrium molecular alignment in turn depends on the anchoring properties of the retaining boundaries (the NLC molecules have a preferred alignment at bounding surfaces), and on applied external fields (electric, in the present application). A thin film of NLC contained between two walls, $\tilde{z} = 0$, $\tilde{z} = \tilde{h}$, say, can be exposed to an electric field; and varying the field across the sample can then change the optical properties in a predictable way. The local alignment of the NLC molecules is described by a unit vector, the *director field*, which gives the average direction of the molecules at a given point.

A drawback of most display devices currently in use is that the molecular alignment created by a particular electric field does not persist once the field is removed. The electric field must therefore be either maintained for as long as the alignment is needed, or electrical pulses applied sufficiently frequently that the optical properties are sustained. Most devices use the latter option, and are made up of an array of 'cells', each cell corresponding to a pixel in the display. An electric field is applied across each cell in turn, until the whole screen has been covered, then the cycle is repeated. Since this takes time, and the molecular alignment rapidly relaxes from the desired configuration, the number of pixels that can be accommodated on a screen is limited, which means that the optical quality of the device is limited.

One idea to permit devices with many pixels is to design a cell that can sustain two (or preferably more) optically-distinct molecular alignments of the NLC that are locally stable in the absence of an electric field (that is, they represent local minima of the system's free energy). To be useful, the NLC must be able to retain the stable configurations until an electric field (or other destabilising effect) is applied, and must also be able to be 'switched' from one such state to the other by application of a suitable electric field. Since only a limited number of pixels are actually required to change in a given 'cycle' of the electric field across the screen, those that are not to be changed can be skipped, speeding up each cycle considerably, as well as lowering power consumption.

Bistable devices are also very important for applications such as 'electronic paper', in which the display is intended to sustain the same format for some length of time. Once the display has been set in the desired configuration, no further electricity should be required to maintain it (though a field can be used to re-set it if necessary).

Bistability may be achieved by, for example, using a specially-shaped cell, in which the NLC is contained between surfaces of given topography. This is the principle behind the Zenithal Bistable nematic Device (ZBD) [4] and the Post-Aligned Bistable nematic Device (PABD) [32, 33]. Because the liquid crystal molecules have a preferred alignment at bounding surfaces, the shape chosen for the surface will also affect the orientation of the director field within the NLC; and, if chosen suitably, can sustain two stable configurations. The BiNem device, described in Dozov & Martinot-Lagarde [11], operates on a different principle. An applied electric field is used to break the weak anchoring at one of the cell boundaries (the director is strongly anchored at the other boundary), leading to flow effects that switch the cell between a 'uniform' and a 'twisted' state.

The basic set-up we shall consider is a thin film of NLC bounded by rigid walls at $\tilde{z} = 0$ and $\tilde{z} = \tilde{h}$. Planes $\tilde{z}$ =constant correspond to the plane of the display (the 'paper', or screen). We shall use overtildes throughout to denote dimensional variables, and drop these when we nondimensionalise.

In § 2 we write down a model for this scenario allowing for the application of a uniform electric field $\boldsymbol{E}$ at arbitrary angle of orientation. In practice an angled (though non-uniform) field could, for example, be realised by offsetting the electrodes so that they do not lie directly opposite each other across the cell. In § 3 we investigate steady states of the model, and their stability, at zero electric field finding at least two stable steady states; two of which lie at a global minimum of the free energy. We proceed in § 4 to continue the zero-field steady solutions to non-zero fields. Here we are interested to see whether

it is possible to switch from zero-field stable solution 1 to zero-field stable solution 2 by gradually increasing the field (from zero) until the solution branch containing solution 1 ceases to exist, thus forcing a jump to that containing solution 2, after which the field is gradually decreased to zero and the solution approaches zero-field stable solution 2. In practice gradual two-way switching, using this device, from $1 \rightarrow 2$ and back from $2 \rightarrow 1$, does not appear possible where the field is applied perpendicular to the cell (the standard practice in switching devices). However it is possible (depending upon material parameters, etc.) where there is a component of field parallel to the cell. This motivates us (in § 5) to investigate whether two way switching between states might be achieved by using a more impulsive application of electric field. Depending upon the material parameters of the liquid crystal and the anchoring energies this is found to be possible even in the case where $\boldsymbol{E}$ is applied normal to the cell.

2 The model

Nematic liquid crystals may be thought of as anisotropic fluids that are (typically) made up of rod-like molecules, which have a local preferred average direction. The long axes of the molecules tend to align parallel to each other along the *anisotropic axis* of the liquid crystal. Mathematically, this may be represented in an idealised way by a *director field* $\boldsymbol{n}$, a unit vector, which describes the orientation of the anisotropic axis in the liquid crystal (the local average preferred direction of the liquid molecules). The evolution of $\boldsymbol{n}$ is then dictated by elastic stresses within the NLC, by the local flow-field, and by externally-acting fields. The mathematical model we shall use is based on the nematic continuum theory due to Ericksen [12] and Leslie [15, 16].

States $-\boldsymbol{n}$ and $\boldsymbol{n}$ are indistinguishable in the theory. We consider the two-dimensional problem in which the unit vector $\boldsymbol{n}$ may be written as

$$\boldsymbol{n} = (\sin\theta, 0, \cos\theta), \tag{2.1}$$

for some function $\theta(\tilde{\boldsymbol{x}}, \tilde{t})$, the angle the director makes with the positive $\tilde{z}$-axis. We make several further simplifying assumptions, the implications of which are discussed further in § 6.

(1) The electric field across the sample is uniform, given by $\tilde{\boldsymbol{E}} = \tilde{E}(\sin\beta\boldsymbol{e}_x + \cos\beta\boldsymbol{e}_z)$ throughout, where $\tilde{E}$ is constant and $\boldsymbol{e}_x$, $\boldsymbol{e}_z$ are the unit vectors in the $\tilde{x}$- and $\tilde{z}$-directions. In reality, both dielectric and flexoelectric effects within the liquid crystal affect the applied electric field, leading to a much harder coupled problem that in general requires numerical solution, even for the static case.

(2) The sample does not vary in the $\tilde{x}$-direction. Thus, we consider a one-dimensional problem in which properties depend only on $\tilde{z}$.

(3) We assume equal elastic constants $\tilde{K}_1$ and $\tilde{K}_3$ in the expression for the elastic energy of the NLC (see (2.3) below). This is not true in general, but the constants are of similar magnitude, and it is a very common assumption in NLC modelling [8, 35].

Stable director configurations are found at minima of the free energy per unit area, $\tilde{J}$, which has both bulk and surface contributions. We write

$$\tilde{J} = \int_0^{\tilde{h}} \tilde{W}\, d\tilde{z} + \tilde{g}|_{\tilde{z}=0} + \tilde{g}|_{\tilde{z}=\tilde{h}}, \tag{2.2}$$

where $\tilde{W}$ is the bulk energy density and $\tilde{g}$ is the surface energy density. When an electric field is present, the bulk energy density is the sum of the elastic, flexoelectric and dielectric energy densities, $\tilde{W}_e$, $\tilde{W}_f$ and $\tilde{W}_d$ respectively. These are defined in terms of the director field and the electric field by:

$$2\tilde{W}_e = \tilde{K}_1(\tilde{\nabla}\cdot\boldsymbol{n})^2 + \tilde{K}_2(\boldsymbol{n}\cdot\tilde{\nabla}\wedge\boldsymbol{n})^2 + \tilde{K}_3\big((\tilde{\nabla}\wedge\boldsymbol{n})\wedge\boldsymbol{n}\big)^2, \tag{2.3}$$

$$\tilde{W}_f = -\tilde{\boldsymbol{E}}\cdot\big(\tilde{e}_1(\tilde{\nabla}\cdot\boldsymbol{n})\boldsymbol{n} + \tilde{e}_3(\tilde{\nabla}\wedge\boldsymbol{n})\wedge\boldsymbol{n}\big), \tag{2.4}$$

$$2\tilde{W}_d = -\tilde{\varepsilon}_0\varepsilon_\perp\tilde{\boldsymbol{E}}\cdot\tilde{\boldsymbol{E}} - \tilde{\varepsilon}_0(\varepsilon_\parallel - \varepsilon_\perp)\big(\boldsymbol{n}\cdot\tilde{\boldsymbol{E}}\big)^2, \tag{2.5}$$

where the $\tilde{K}_i$ are elastic constants; $\tilde{e}_1$ and $\tilde{e}_3$ are flexoelectric coefficients; $\tilde{\varepsilon}_0$ is the permittivity of free space; and $\varepsilon_\parallel$ and $\varepsilon_\perp$ are the relative dielectric permittivities parallel and perpendicular to the long axis of the molecules. The terms in $\tilde{K}_1$, $\tilde{K}_2$ and $\tilde{K}_3$ represent 'splay', 'twist' and 'bend' of the director field, respectively (see elsewhere [8, 35] for a physical interpretation). In general for problems with weak anchoring one should include an extra 'saddle-splay' term [35], usually written as $(\tilde{K}_2+\tilde{K}_4)\tilde{\nabla}\cdot[(\boldsymbol{n}\cdot\tilde{\nabla})\boldsymbol{n}-(\tilde{\nabla}\cdot\boldsymbol{n})\boldsymbol{n}]$, in the elastic energy (2.3); however with our two-dimensional assumption ((2.1) and point 2 above) this contribution vanishes identically.

The term $\big(\tilde{e}_1(\tilde{\nabla}\cdot\boldsymbol{n})\boldsymbol{n} + \tilde{e}_3(\tilde{\nabla}\wedge\boldsymbol{n})\wedge\boldsymbol{n}\big)$ occurring in $\tilde{W}_f$ is the *flexoelectric polarisation* [8, 35] of the NLC molecules, due to the fact that they are asymmetric and contain a small permanent electric dipole.

The form of the surface energy, $\tilde{g}$, is chosen to mimic the fact that the NLC molecules at a boundary have a preferred direction (which depends on the properties of the boundary, and may be altered by treating the boundary [8, 25]). The assumption we make to obtain bistability is that the anchoring at the upper and lower surfaces is $\pi/2$ out of phase: if α is the preferred director alignment at the lower surface, then $(\alpha - \pi/2)$ is the preferred alignment at the upper surface. Thus, using the usual Rapini-Papoular [24] formula for surface energy, we have $\tilde{g}_+ = (\tilde{A}/2)\cos^2(\theta-\alpha)$, $\tilde{g}_- = (\tilde{A}/2)\sin^2(\theta-\alpha)$, where $\tilde{A}$ is the anchoring strength at either surface.

Much liquid crystal research is devoted to the creation of "designer" surfaces with (stable) specified anchoring properties, and much progress has been made in this direction [6, 13, 25, 30, 31]. By suitable treatments it is now possible to engineer a surface at which the NLC molecules have a large, predictable, polar pretilt angle (the anchoring angle α) [25, 30].

2.1 Scaling and nondimensionalisation

Scaling $\tilde{z}$ with the cell height $\tilde{h}$, $\tilde{z} = \tilde{h}z$, then with the equal-elastic constants assumption $\tilde{K}_1 = \tilde{K}_3 = \tilde{K}$ in (2.3), the total energy density within the bulk is found (to within an

additive constant) to be given by

$$\tilde{W} = \frac{\tilde{K}}{\tilde{h}^2}\left\{\frac{\theta_z^2}{2} + \frac{\mathscr{F}\theta_z}{2}\big(\sin(2\theta-\beta) + (\hat{e}_1 - \hat{e}_3)\sin\beta\big) - \mathscr{D}\cos^2(\theta-\beta)\right\}$$
$$\equiv \frac{\tilde{K}W}{\tilde{h}^2}, \tag{2.6}$$

(the second equality defines the dimensionless leading order bulk energy density W). The dimensionless parameters $\mathscr{F}$ and $\mathscr{D}$ are given by

$$\mathscr{F} = \frac{\tilde{h}\tilde{E}(\tilde{e}_1 + \tilde{e}_3)}{\tilde{K}}, \qquad \mathscr{D} = \frac{\tilde{h}^2\tilde{E}^2\tilde{\varepsilon}_0\varepsilon_a}{2\tilde{K}}; \tag{2.7}$$

$\mathscr{F}$ may be considered as a dimensionless electric field, or as a measure of the strength of the flexoelectric effect relative to elasticity in the problem, while $\mathscr{D}$ measures dielectric effects. The normalised flexoelectric coefficients $\hat{e}_1$ and $\hat{e}_3$ are defined by $\hat{e}_i = \tilde{e}_i/(\tilde{e}_1 + \tilde{e}_3)$ $i = 1, 3$, and the dielectric anisotropy $\varepsilon_a = \varepsilon_\parallel - \varepsilon_\perp$. The results of Murthy *et al.* [20] suggest that $(\tilde{e}_1 + \tilde{e}_3)$ will probably be positive. Given the characteristic values

$$\tilde{h} \sim 1\mu\text{m}, \quad \tilde{E} \sim 1\text{V}\mu\text{m}^{-1}, \quad \tilde{e}_1 + \tilde{e}_3 \sim 0.5 \times 10^{-10}\text{C m}^{-1},$$
$$\tilde{K} \sim 1 \times 10^{-11}\text{N}, \quad \tilde{\varepsilon}_0 = 8.854 \times 10^{-12}\text{C}^2\text{N}^{-1}\text{m}^{-2}, \quad \varepsilon_a \sim O(1)$$

[2], $|\mathscr{F}|$ and $\mathscr{D}$ are seen to be roughly of order unity.

The sign of $\mathscr{F}$ is dictated by the direction of the electric field, while $\mathscr{D}$ will have the same sign as ε_a, which can be either positive or negative, but is a material property of the NLC used. Thus, in a particular application we can change the sign of $\mathscr{F}$ by reversing the electric field, but the sign of $\mathscr{D}$ is fixed. The ratio $\mathscr{F}^2/\mathscr{D}$ is independent of the applied electric field. We define

$$\Upsilon = \frac{\mathscr{F}^2}{\mathscr{D}} = \frac{2(\tilde{e}_1 + \tilde{e}_3)^2}{\tilde{K}\tilde{\varepsilon}_0\varepsilon_a}; \tag{2.8}$$

this will be an important material parameter in the problem. We may then identify the leading-order dimensionless free energy J per unit area as

$$J = \int_0^1 W\,dz + g_-|_{z=0} + g_+|_{z=1}, \tag{2.9}$$

where $\tilde{g}_\pm = \tilde{K}g_\pm/\tilde{h}$ defines the dimensionless surface energy $g_\pm$, given by

$$g_+ = \frac{A}{2}\cos^2(\theta-\alpha), \qquad g_- = \frac{A}{2}\sin^2(\theta-\alpha), \qquad A = \tilde{h}\tilde{A}/\tilde{K}. \tag{2.10}$$

2.2 Static solutions

Possible static configurations of the liquid crystal are given by stationary values of the free energy, stable static configurations being at local minima of the free energy. The standard Euler-Lagrange approach for identifying such static solutions $\theta(z)$ is to consider the variation induced in the energy J by small variations in θ: $\theta(z) \mapsto \theta(z) + \epsilon\eta(z)$,

where $0 < \epsilon \ll 1$. Considering J as a functional of θ (and its partial derivatives) we may compute its first and second variations, that is, the order-ϵ and order-ϵ^2 terms in $\Delta J := J[\theta + \epsilon\eta] - J[\theta]$. We find

$$\Delta J = \epsilon \int_0^1 \eta[W_\theta - (W_{\theta_z})_z]dz + \epsilon\eta\big(g_\theta + W_{\theta_z}\big)_{z=1} + \epsilon\eta\big(g_\theta - W_{\theta_z}\big)_{z=0} + \frac{\epsilon^2}{2}\int_0^1 \{\eta^2[W_{\theta\theta} - (W_{\theta\theta_z})_z] + \eta_z^2 W_{\theta_z\theta_z}\}dz + \frac{\epsilon^2}{2}\eta^2\big(g_{\theta\theta} + W_{\theta\theta_z}\big)_{z=1} + \frac{\epsilon^2}{2}\eta^2\big(g_{\theta\theta} - W_{\theta\theta_z}\big)_{z=0} + O(\epsilon^3). \tag{2.11}$$

The first variation must vanish at an equilibrium solution for all admissible (sufficiently smooth) variations η. Hence using (2.6), the integral at order ϵ gives

$$\theta_{zz} = \mathscr{D}\sin(2\theta - 2\beta) \quad 0 < z < 1, \tag{2.12}$$

and using (2.10) the boundary terms at this order yield

$$\theta_z - \frac{A}{2}\sin(2\theta - 2\alpha) + \frac{\mathscr{F}}{2}\big[\sin(2\theta - \beta) + (\hat{e}_1 - \hat{e}_3)\sin\beta\big] = 0 \text{ on } z = 0,\ 1. \tag{2.13}$$

Note that the flexoelectric term enters static solutions only via the boundary condition on θ. It will, however, affect solution stability, which is determined by consideration of the second variation. Writing this as $(\Delta J)_2$, we find

$$(\Delta J)_2 = \frac{\epsilon^2}{2}\int_0^1 \big[\eta_z^2 + 2\eta^2\mathscr{D}\cos(2\theta - 2\beta)\big]\,dz - \frac{\epsilon^2}{2}\big[\eta^2\,(A\cos(2\theta - 2\alpha) - \mathscr{F}\cos(2\theta - \beta))\big]_0^1. \tag{2.14}$$

If $(\Delta J)_2 > 0$ for all admissible variations η, then small variations in θ (satisfying (2.12), (2.13)) increase the energy, and the solution is stable. But if there exist variations for which $(\Delta J)_2 < 0$ then the solution is unstable, as one can decrease the energy by suitable small changes in θ.

2.3 Time-dependent solutions

The above applies only to static solutions. Starting from the Ericksen-Leslie equations [12, 16,17] and assuming that flow effects are negligible, it may be shown that time-dependent solutions will relax to a solution of (2.12, 2.13) via the partial differential equation

$$\theta_t = \theta_{zz} - \mathscr{D}\sin(2\theta - 2\beta) \quad 0 < z < 1. \tag{2.15}$$

This is solved subject to boundary conditions that are similar to those for the static case, but modified by the inclusion of a surface dissipation,

$$\pm\nu\theta_t = \theta_z - \frac{A}{2}\sin(2\theta - 2\alpha) + \frac{\mathscr{F}}{2}\big(\sin(2\theta - \beta) + (\hat{e}_1 - \hat{e}_3)\sin\beta\big) \quad \text{on } z = 0,\ 1. \tag{2.16}$$

This was the approach taken by Kedney & Leslie [14] and Davidson & Mottram [7] in solving closely-related problems. In (2.15, 2.16) time has been made dimensionless by scaling with $\tilde{\mu}\tilde{h}^2/\tilde{K}$, where $\tilde{\mu}$ is a "viscosity" associated with director rotation: $\tilde{t} = t\tilde{\mu}\tilde{h}^2/\tilde{K}$. The parameter v is given by $v = \tilde{v}/(\tilde{\mu}\tilde{h})$, where $\tilde{v}$ is a surface relaxation coefficient [7, 14]. It is often written in terms of the surface viscosity $\tilde{\mu}$ via $\tilde{v} = \gamma\tilde{\mu}$, where γ is a surface length, thought to be of the order of the molecular length (see [7]). Thus, $v = \gamma/\tilde{h}$ will be order 1 or smaller in our problem.

3 Solutions and stability with no electric field

We seek multiple steady solutions to (2.12) and (2.13) that are stable in the absence of an applied field: $\mathscr{D} = 0 = \mathscr{F}$. Thus

$$\theta = az + b, \tag{3.1}$$

where the constants a and b satisfy

$$a = \frac{A}{2}\sin(2a + 2b - 2\alpha), \quad a = \frac{A}{2}\sin(2b - 2\alpha). \tag{3.2}$$

Subtracting equations (3.2) leads to two possibilities:

$$(1) \quad \sin a = 0 \quad \text{or} \quad (2) \quad \cos(a + 2b - 2\alpha) = 0. \tag{3.3}$$

Case (1): $a = k\pi$ for some integer k, and b is then determined by either of equations (3.2). For $A < 2\pi$ then, there are only two solutions for b (modulo π), namely

$$1(\text{i}) \quad a = 0,\ b = \alpha, \quad \text{or } 1(\text{ii}) \quad a = 0,\ b = \alpha + \frac{\pi}{2}.$$

Stability of such solutions is determined by the boundary contributions to the 2nd variation $(\Delta J)_2$ (2.14), since the bulk contribution is always positive. Since $a = k\pi$, we have

$$\cos(2\theta - 2\alpha)|_{z=1} = \cos(2b - 2\alpha) = \cos(2\theta - 2\alpha)|_{z=0}.$$

Thus, the two boundary contributions to $(\Delta J)_2$ are of opposite sign, meaning that $(\Delta J)_2$ can be made negative by choice of a suitable variation η (a linear function of z will do). It follows that such solutions cannot represent local energy minima, hence they are unstable.

Case (2): There are two sub-cases here,

$$2(\text{i}) \quad \sin(a + 2b - 2\alpha) = 1 \quad \text{or } 2(\text{ii}) \quad \sin(a + 2b - 2\alpha) = -1,$$

giving

$$2(\text{i}) \quad a + 2b - 2\alpha = 2k\pi + \frac{\pi}{2} \quad \text{or } 2(\text{ii}) \quad a + 2b - 2\alpha = 2k\pi + \frac{3\pi}{2},$$

for some integer k. It follows that

$$\sin(2b - 2\alpha) = \begin{cases} \cos a & \text{case 2(i)} \\ -\cos a & \text{case 2(ii)}, \end{cases}$$

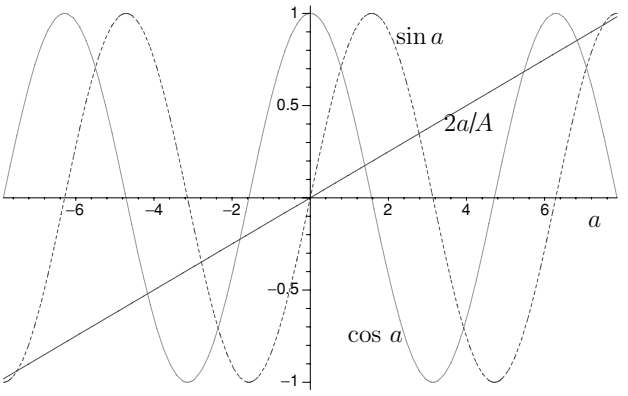

FIGURE 1. Figure showing the location of the roots of $a = (A/2)\cos a$, (solutions of type 2(i); intersections of solid curves) which are stable if the dotted curve $\sin a$ is positive, and unstable otherwise.

and thus, by the second of equations (3.2), a satisfies

$$a = \begin{cases} \frac{A}{2}\cos a & \text{case 2(i)} \\ -\frac{A}{2}\cos a & \text{case 2(ii)}, \end{cases} \tag{3.4}$$

with

$$b = \begin{cases} \alpha - \frac{a}{2} + \frac{\pi}{4} & \text{(modulo } \pi\text{) case 2(i)} \\ \alpha - \frac{a}{2} + \frac{3\pi}{4} & \text{(modulo } \pi\text{) case 2(ii).} \end{cases} \tag{3.5}$$

The 2nd variation for these solutions is given by

$$(\Delta J)_2 = \frac{\epsilon^2}{2}\int_0^1 \eta_z^2\, dz \pm \frac{\epsilon^2}{2}\, A\eta^2 \sin a\big|_{z=0} \pm \frac{\epsilon^2}{2}\, A\eta^2 \sin a\big|_{z=1} \tag{3.6}$$

the (+) sign for case 2(i) and the (−) sign for case 2(ii); thus case 2(i) solutions are stable if $\sin a > 0$, and case 2(ii) solutions are stable if $\sin a < 0$. The general situation in case 2(i) is sketched in Figure 1, which shows the graphs of $y = \cos a$ and $y = 2a/A$ (solid lines), the intersections of which correspond to steady solutions of type 2(i). The dotted curve is $y = \sin a$, the sign of which determines the stability of a given steady solution (positive ⇒ stable; negative ⇒ unstable). An analogous figure may be plotted for case 2(ii), in which the sign of $(-\sin a)$ determines the stability of a given steady solution (positive ⇒ stable; negative ⇒ unstable).

In each case there is a stable root a of smallest magnitude; $a_1 > 0$ for case 2(i), and $a_2 \equiv -a_1$ for case 2(ii). There may be other stable roots (as Figure 1 shows), depending on the size of A, but the solutions a_1 and a_2 always exist, and will be of lower energy than any other possible stable solutions in the two cases. The director angle θ in these cases is (modulo π)

$$\theta_1 = a_1 z + \alpha - \frac{a_1}{2} + \frac{\pi}{4}, \tag{3.7}$$

$$\theta_2 = -a_1 z + \alpha + \frac{a_1}{2} + \frac{3\pi}{4} \equiv -\theta_1 + 2\alpha, \tag{3.8}$$

where a_1 is the smallest positive root of $a_1 = (A/2)\cos a_1$, and we write $\boldsymbol{n}_1 = (\sin\theta_1, 0, \cos\theta_1)$, $\boldsymbol{n}_2 = (\sin\theta_2, 0, \cos\theta_2)$ for the director solutions. They have associated energies J defined by (2.9), in which it is easily seen that $W = a_1^2/2$, and $g_\pm = (A/4)(1-\sin a_1)$ for both cases, so that the two stable steady solutions are of equal energy.

Changing the pretilt angle α simply translates the director angle θ (a straightforward rotation of $\boldsymbol{n}_1$ or $\boldsymbol{n}_2$ within the cell), while changing the anchoring strength changes the angle a_1 that the director rotates through across the cell. Lowering the anchoring strength reduces this angle, as the substrates have less influence on the director orientation.

4 Solutions and stability with an electric field

In this section we investigate possible switching mechanisms using a time-independent bifurcation analysis. The advantage of this approach, rather than considering a time-dependent model (as we do later), is that the steady state model of liquid crystals has a firmer physical foundation than the time-dependent model and there is far more data available for the parameters in the steady state model. However, this approach has the disadvantage that we cannot investigate the effects of a particular switching regime. Our approach throughout this section is to continue the known static solutions at zero electric field to non-zero fields using the continuation package Auto 97 [10]. It is then possible to infer the stability of the continued solutions from their stability at zero field, which was derived in § 3. In particular we shall use the fact that the stability of a solution branch does not change until a fold or bifurcation is reached (a stable solution branch necessarily loses stability after passing through a fold). This will enable us to deduce the stability of all solution branches (and sections thereof) in what follows.

We first write (2.12) and (2.13) in terms of the dimensionless parameter $\mathscr{F}$ introduced in (2.7) (which we here interpret as a dimensionless electric field); and the dimensionless material parameter Υ (which will be constant for any given NLC that we might use in a device), defined in (2.8). In terms of these the steady equations are

$$\theta_{zz} = \frac{\mathscr{F}^2}{\Upsilon}\sin(2\theta - 2\beta) \qquad 0 < z < 1, \tag{4.1}$$

$$\theta_z = \frac{A}{2}\sin(2\theta - 2\alpha) - \frac{\mathscr{F}}{2}\left[\sin(2\theta - \beta) + (\hat{e}_1 - \hat{e}_3)\sin\beta\right] \quad \text{on } z = 0, 1 \tag{4.2}$$

and the dimensionless free energy per unit area J (defined in (2.9)) is

$$\begin{aligned} J = &\int_0^1 \theta_z^2 dz - \frac{\mathscr{F}^2}{2\Upsilon} - \frac{1}{2}\left(\theta_z^2 + \frac{\mathscr{F}^2}{\Upsilon}\cos(2\theta - 2\beta)\right)\Big|_{z=1} \\ &+ \frac{\mathscr{F}}{2}\left[\theta(\hat{e}_1 - \hat{e}_3)\sin\beta - \frac{\cos(2\theta - \beta)}{2}\right]_0^1 \\ &+ \frac{A}{2} + \frac{A}{4}\left(\cos(2\theta - 2\alpha)|_{z=1} - \cos(2\theta - 2\alpha)|_{z=0}\right), \end{aligned} \tag{4.3}$$

where we have written J in a form that is easy to plot using AUTO 97.[1]

[1] Multiply (4.1) by θ_z and integrate with respect to z to find an expression for $\cos(2\theta - 2\beta)$. Then use this to express $\int_0^1 \cos^2(\theta - \beta)$ in terms of $\int_0^1 \theta_z^2 dz$ and boundary terms.

Note that (4.1) can be integrated to give an explicit solution for θ in terms of elliptic integrals (see, for example, Davidson & Mottram [7]). However, applying the nonlinear boundary condition (4.2) gives rise to a transcendental equation for the arbitrary constants in the general solution for θ, which is nontrivial to solve. It turns out to be as easy to solve the boundary value problem for θ numerically, and this is the approach we take. We shall concentrate on the special case $\alpha = \pi/3$ since the two corresponding stable $\mathscr{F} = 0$ static solutions would be optically distinct in a display device. The size of A (the dimensionless surface energy parameter) determines to a large extent whether it is possible to switch out of one state to another using the flexoelectric effect: if A becomes too large switching is impossible, essentially because the energy wells that the stable steady states lie in are too deep to be significantly perturbed by flexoelectricity.

4.1 Order-one surface energy: $A = 1$

We look first at $A = 1$ and investigate the effects of changing the material parameter Υ, defined in (2.8), and the electric field orientation β.

(i) $\beta = 0$**.**
This is the case in most display devices currently in use, with the electric field applied perpendicular to the 'screen'. Note first that (4.1)-(4.2) are invariant under

$$\Upsilon \to -\Upsilon, \qquad \theta \to \theta + \pi/2, \qquad z \to 1 - z, \tag{4.4}$$

so we need only consider $\Upsilon \geqslant 0$. Secondly the $\mathscr{F} = 0$ steady solutions found earlier are $\theta = ax + b + n\pi$, where n is an integer, and

1(i)	$(a, b) = (0, \pi/3)$	unstable,
1(ii)	$(a, b) = (0, 5\pi/6)$	unstable,
2(i)	$(a, b) = (0.450, 1.608)$	stable,
2(ii)	$(a, b) = (-0.450, 3.628)$	stable.

It is convenient to plot the solution branches in $(\mathscr{F}, \|\theta\|_2)$-parameter space, where we use $\|\cdot\|_2$ to denote the L_2-norm of θ:

$$\|\theta\|_2 = \sqrt{\int_0^1 \theta^2 dz}.$$

In this instance, as Υ is decreased, a transition is made from a scenario in which there are 4 solution branches in $(\mathscr{F}, \|\theta\|_2)$-parameter space (exemplified by the case $\Upsilon = 36$ in Figure 2(A)) to one in which there are 2 unfolded branches and 1 folded branch (as in Figure 2(B) with $\Upsilon = 4$) to the case in which there are two folded solution branches (as in Figure 2(C) with $\Upsilon = 1$). Decreasing Υ means that the effect of flexoelectricity relative to elasticity within the liquid crystal is decreased.

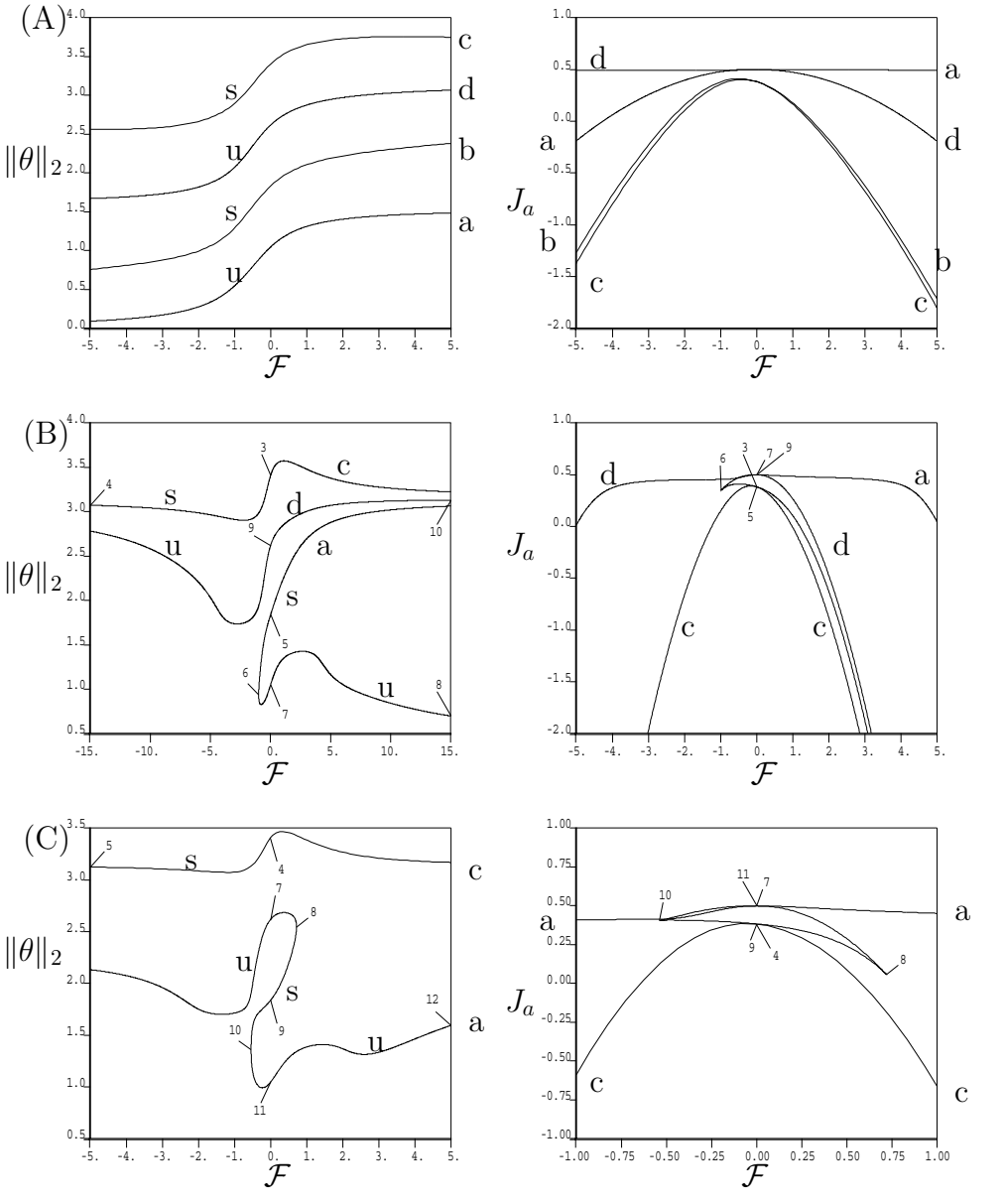

FIGURE 2. Bifurcation diagrams for $\alpha = \pi/3$, $A = 1$, $\beta = 0$, with: (A) $\Upsilon = 36$, (B) $\Upsilon = 4$ and (C) $\Upsilon = 1$. Stability of bifurcation curves is indicated by (s) stable or (u) unstable. Curves are labelled 'a'–'d' to identify the corresponding energy curves, and additionally in (B) and (C) numbers are used to match special points on the bifurcation curve with the corresponding points on the energy curves. In (A) the steady solution (at $\mathscr{F} = 0$) 1(i) lies on 'a', 1(ii) on 'd', 2(i) on 'b' and 2(ii) on 'c'. In (B), 1(i) lies at point 7, 1(ii) lies at 9, 2(i) lies at 5 and 2(ii) lies at 3. In (C) 1(i) lies at 11, 1(ii) at 7, 2(i) at 9 and 2(ii) at 4.

In the first case $\Upsilon = 36$ (Figure 2(A)) there are two stable solution curves ('b' and 'c') interlaced by 2 unstable curves ('a' and 'd'). The energies of the stable curves (also plotted) are very similar, with that of 'c' (the branch of global minimum energy) being slightly lower than that of 'b'. This hints that it may be possible to switch from 2(i) (which lies on 'b') to 2(ii) (which lies on 'c'), and vice-versa, by a judicious choice of switching protocol. A major problem in switching from a stable branch of global minimum energy (such as 'c') to another stable branch with higher energy (such as 'b') is that the basin of attraction surrounding the latter is usually smaller (and thus more difficult to target) than that of global minimum energy. A small energy difference between the two branches might thus be expected to favour such switching; and as the time-dependent simulations that follow show, such switching from branch 'c' into 'b' is possible. In the third case $\Upsilon = 1$ (Figure 2(C)) the two unstable $\mathscr{F} = 0$ solutions (1(i) and 1(ii)) are linked through a folded curve in $(\mathscr{F}, \|\theta\|_2)$-parameter space to the stable $\mathscr{F} = 0$ solution 2(i). Since solution stability can only change at a fold or bifurcation, it follows that the segment of curve with point 9 on it is stable. Furthermore, for $\mathscr{F} > 0.72$ (or $\mathscr{F} < -0.54$) this stable solution branch ceases to exist, and one would therefore expect the solution to jump to the other stable branch, labelled 'c', on which 2(ii) lies. It should be relatively easy, therefore, to switch from solution 2(i) to 2(ii) simply by increasing/decreasing the field sufficiently, and then lowering it back to zero again. However, no such technique can be used to switch from 2(ii) to 2(i). In addition, the energies of curve 'c' and curve 'a', which are also shown in Figure 2, diverge rapidly away from $\mathscr{F} = 0$, with 'c' taking lower energy values than 'a', suggesting that switching from a solution on 'c' to one on 'a' may be difficult (it was not found possible for this value of Υ in our time-dependent simulations; see Figures 5, 7 and 8 later).

Likewise, in the intermediate case $\Upsilon = 4$ (Figure 2(B)), switching from the stable solution 2(i) (on the upper branch of the folded curve 'a') to the stable solution 2(ii) (on curve 'c') is easily achieved by lowering the field to below the fold point, before increasing it to zero again. However switching from the stable solution 2(ii) is problematic, as no fold (or bifurcation) exists on its solution branch.

(ii) $\beta = \pi/4$**,** $(\hat{e}_1 - \hat{e}_3) = 1/2$**.**

Given that there is no foolproof switching mechanism when the electric field is applied normal to the liquid crystal cell ($\beta = 0$), we investigate a case in which it is applied at an angle to the cell (we look at $\beta = \pi/4$). An extra parameter $(\hat{e}_1 - \hat{e}_3)$ now appears in the boundary conditions (4.2), and must be specified. Assuming (based on earlier data [5,20]) that the 'splay' flexoelectric coefficient $\tilde{e}_1$ is larger than the 'bend' flexoelectric coefficient $\tilde{e}_3$, we set $(\hat{e}_1 - \hat{e}_3) = 0.5$ in the following.

The dielectric term $-(\mathscr{F}^2/\Upsilon)\cos^2(\theta - \beta)$ in the energy acts to align θ with β where $\Upsilon > 0$, and perpendicular to β where $\Upsilon < 0$. The steady state 2(i) lies much closer to $\theta = \pi/4$ than does 2(ii), thus we expect the choice of $\beta = \pi/4$ to make switching from state 2(ii) to 2(i) easier (with $\Upsilon > 0$) than in the case $\beta = 0$, and switching in the reverse direction more difficult.

Bifurcation diagrams for $\beta = \pi/4$ for various values of Υ, and the corresponding energy plots, are shown in Figures 3-4. Here it is convenient to plot solution branches in

$(\mathscr{F}, \|\theta\|)$-space, where the norm $\|\cdot\|$ is defined by

$$\|\theta\| = \int_0^1 \theta dz.$$

This is π-periodic, since θ is itself π-periodic. As Υ decreases, a transition is made from a scenario in which there are two singly-folded solution branches (e.g. $\Upsilon = 4$, in Figure 3(A)) to one in which there is a doubly-folded solution branch and an unfolded branch (e.g. $\Upsilon = 1$, in Figure 3(B)), to one in which one of the branches is a closed loop and the other 2 are unfolded (Figures 3(C) and (D)). Note that for the $\Upsilon = 1$ case (Figure 3(B)), both stable solutions 2(i) and 2(ii) lie on the same branch, separated by an unstable segment.

Where $\Upsilon \gtrapprox 0.305$ (Figures 3(A) and (B)) it is possible to switch from the stable $\mathscr{F} = 0$ solution 2(ii) to 2(i) by decreasing $\mathscr{F}$ below the fold point (on 2(ii)'s solution branch, which is 'a' in both Figures 3(A) and (B)), before increasing $\mathscr{F}$ back to zero again. One can also switch back from 2(i) to 2(ii) by increasing $\mathscr{F}$ above the fold point (on 2(i)'s solution branch; 'b' in Figure 3(A), 'a' in 3(B)) before decreasing it again to zero. This gives an ideal bistable device, which is very easy to switch between its stable states in a manner which is not particularly sensitive to the switching protocol adopted.

For $0 < \Upsilon \lessapprox 0.305$ (Figure 3(D)) it is possible to switch from solution 2(i), on the curve 'a', to 2(ii), on the curve 'c', either by increasing or decreasing the field past a fold point; however, switching the other way from 2(ii) to 2(i) will rely on the precise protocol used.

Figures 4(A) and 4(B) show typical bifurcation diagrams for $\Upsilon < 0$. In both cases there is no obvious way of switching from 2(i) to 2(ii) although in (A) it is clear that switching from 2(ii) to 2(i) will be possible.

4.2 The limit $\Upsilon \to +\infty$, $\mathscr{F} = o(\Upsilon^{1/2})$.

Motivated by the numerical results of §5 below, which suggest that two-way switching between the zero-field stable states may still be possible if the dielectric effect is neglected in our model, we briefly consider this limit in which further analytical progress may be made.[2] To leading order we may neglect the dielectric term in (4.1), formally setting $\theta_{zz} = 0$ so that $\theta = az + b$. Application of boundary conditions (4.2) gives

$$2a - A\sin(2b - 2\alpha) + \mathscr{F}(\sin(2b - \beta) + (\hat{e}_1 - \hat{e}_3)\sin\beta) = 0, \tag{4.5}$$

$$2a - A\sin(2b + 2a - 2\alpha) + \mathscr{F}(\sin(2b + 2a - \beta) + (\hat{e}_1 - \hat{e}_3)\sin\beta) = 0; \tag{4.6}$$

subtracting (4.5) from (4.6) and rearranging then leads to the conclusion that

$$\text{either} \quad (1) \quad \sin a = 0 \quad \text{or} \quad (2) \quad \tan(a + 2b) = \frac{\mathscr{F}\cos\beta - A\cos 2\alpha}{A\sin 2\alpha - \mathscr{F}\sin\beta}. \tag{4.7}$$

Equations (4.5) and (4.6) above comprise a transcendental system for a and b. To solve, it is helpful to introduce the function

$$Q(\mathscr{F}) = \arctan\left(\frac{\mathscr{F}\cos\beta - A\cos 2\alpha}{A\sin 2\alpha - \mathscr{F}\sin\beta}\right),$$

[2] We are grateful to a referee for suggesting this idea.

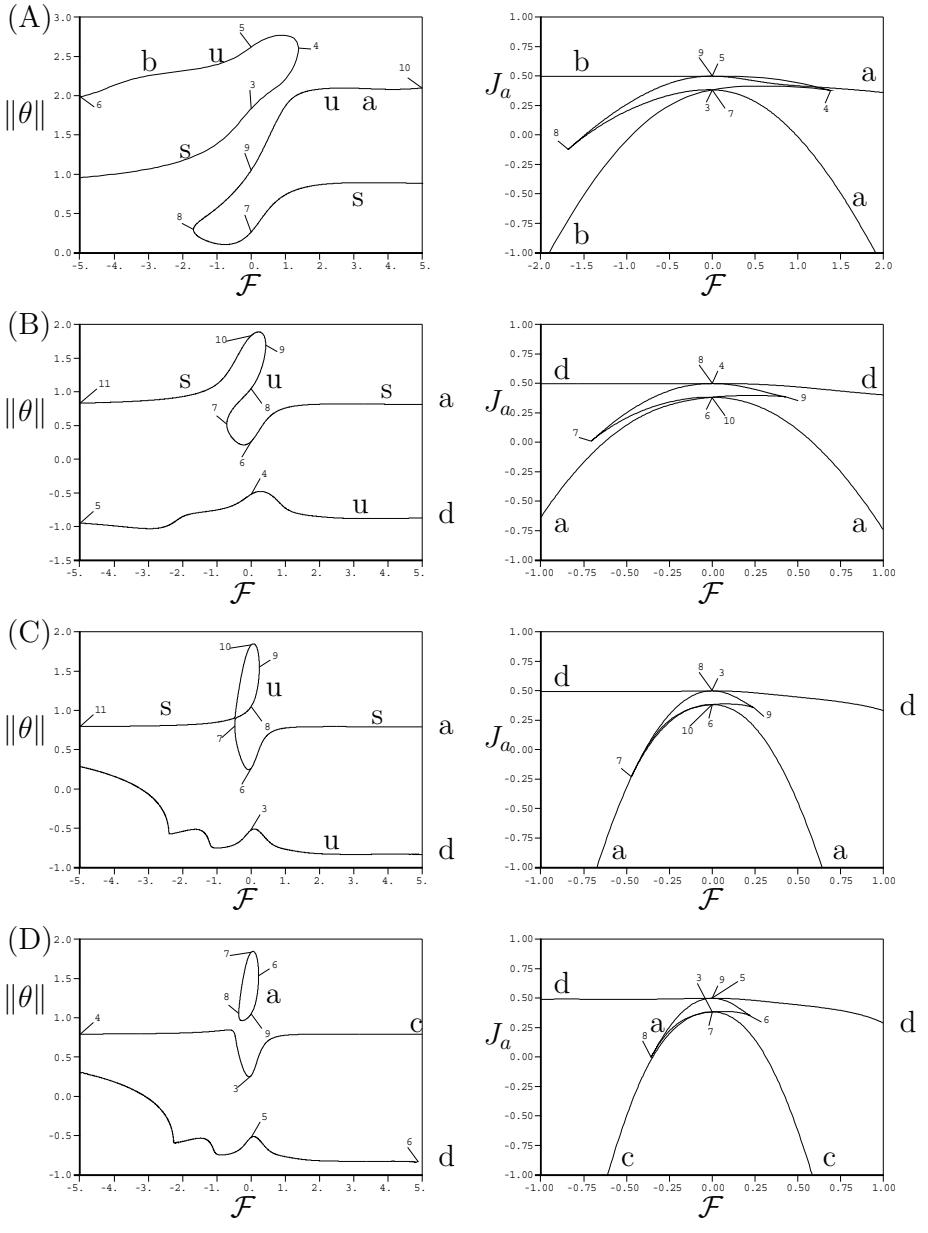

FIGURE 3. Bifurcation diagrams for $\alpha = \pi/3$, $A = 1$, $\beta = \pi/4$, $\hat{e}_1 - \hat{e}_3 = 1/2$, with (A) $\Upsilon = 4.0$, (B) $\Upsilon = 1$, (C) $\Upsilon = 0.305$, (D) $\Upsilon = 0.2$. Numbers are used to identify special points on the bifurcation curve with the corresponding points on the energy curves, in addition to the letters 'a'–'d'. The steady $\mathscr{F} = 0$ solutions in (A): 1(i) lies at 9, 1(ii) at 5, 2(i) at 3 and 2(ii) at 7. In (B): 1(i) lies at 8, 1(ii) at 4, 2(i) at 10 and 2(ii) at 6. (C) as for (B), except 1(ii) lies at point 3. In (D): 1(i) lies at 9, 1(ii) at 5, 2(i) at 7 and 2(ii) at 3.

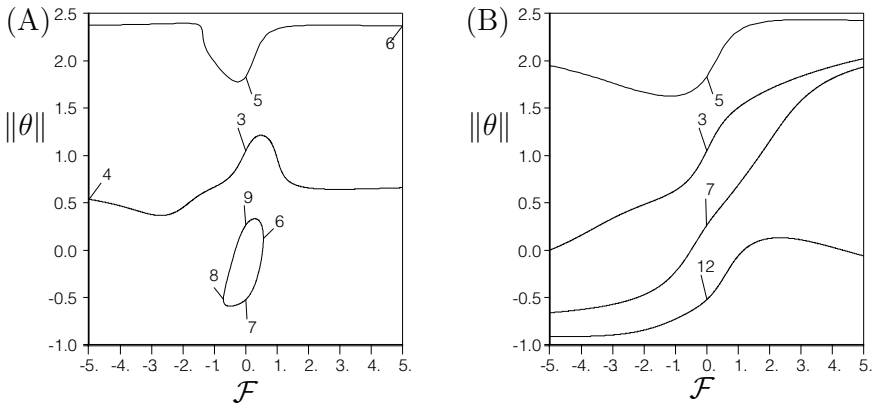

FIGURE 4. Bifurcation diagrams for $\alpha = \pi/3$, $A = 1$ $\beta = \pi/4$, $\hat{e}_1 - \hat{e}_3 = 1/2$, with (A) $\Upsilon = -1$, and (B) $\Upsilon = -4$. Numbers identify special points on the bifurcation curve with the corresponding points on the energy curves, in addition to letters 'a', 'c' and 'd'. In (A) the steady $\mathscr{F} = 0$ solution 1(i) lies at point 3, 1(ii) at 7, 2(i) at 5 and 2(ii) at 9. In (F) 1(i) lies at 3, 1(ii) at 12, 2(i) at 5 and 2(ii) at 7.

in terms of which we can rewrite (4.5) and (4.6) as

$$\text{either} \quad (1) \quad \sin a = 0 \quad \text{or} \quad (2) \quad \tan(a + 2b) = \tan(Q(\mathscr{F})), \tag{4.8}$$

$$\cos(2b - Q(\mathscr{F})) + \frac{(2a/A) + (\mathscr{F}/A)(\hat{e}_1 - \hat{e}_3)\sin\beta}{\left[(\mathscr{F}/A)^2 - 2(\mathscr{F}/A)\cos(2\alpha - \beta) + 1\right]^{1/2}} = 0. \tag{4.9}$$

In case 1 we shall only consider $a = 0$; this leads to two solutions for b

$$1(i)\ b = b_1 \quad \text{or} \quad 1(ii)\ b = b_1 + \frac{\pi}{2}, \quad \text{where}$$
$$b_1 = \frac{Q(\mathscr{F})}{2} + \frac{1}{2}\arccos\left(\frac{-(\mathscr{F}/A)(\hat{e}_1 - \hat{e}_3)\sin\beta}{\left[(\mathscr{F}/A)^2 - 2(\mathscr{F}/A)\cos(2\alpha - \beta) + 1\right]^{1/2}}\right). \tag{4.10}$$

In case 2 we again find two solutions

$$2(i)\begin{cases} \cos a = \dfrac{(2a/A) + (\mathscr{F}/A)(\hat{e}_1 - \hat{e}_3)\sin\beta}{\left[(\mathscr{F}/A)^2 - 2(\mathscr{F}/A)\cos(2\alpha - \beta) + 1\right]^{1/2}}, \\ b = \dfrac{\pi}{2} + \dfrac{Q(\mathscr{F})}{2} - \dfrac{a}{2} + k\pi \end{cases} \tag{4.11}$$

$$2(ii)\begin{cases} \cos a = -\dfrac{(2a/A) + (\mathscr{F}/A)(\hat{e}_1 - \hat{e}_3)\sin\beta}{\left[(\mathscr{F}/A)^2 - 2(\mathscr{F}/A)\cos(2\alpha - \beta) + 1\right]^{1/2}}, \\ b = \pi + \dfrac{Q(\mathscr{F})}{2} - \dfrac{a}{2} + k\pi \end{cases} \tag{4.12}$$

where $k = 0$ if $\alpha \in [0, \pi/2]$ and $k = 1$ if $\alpha \in (-\pi/2, 0)$. The labelling of these solutions corresponds to the steady solutions found in § 3 at $\mathscr{F} = 0$.

Stability

In case 1 the second variation of the energy is given by

$$(\Delta J)_2 = \frac{\epsilon^2}{2}\left\{\int_0^1 \eta_z^2 dz - \left[(A\cos(2b-2\alpha) - \mathscr{F}\cos(2b-\beta))\,\eta^2\right]_0^1\right\}$$

where η is any sufficiently smooth test function; see § 3 (it is not constrained on the boundary). It is easy to show, by taking $\eta = K + Mz$, that it is possible to find functions η for which $(\Delta J)_2 < 0$ for any value of $\mathscr{F}$. It follows that solutions of the form 1 are always unstable.

In case 2

$$(\Delta J)_2 = \frac{\epsilon^2}{2}\left\{\int_0^1 \eta_z^2 dz + (A\cos(2b-2\alpha) - \mathscr{F}\cos(2b-\beta))\,\eta^2\big|_{z=0} - (A\cos(2b+2a-2\alpha) - \mathscr{F}\cos(2b+2a-\beta))\,\eta^2\big|_{z=1}\right\}$$

By using standard trigonometric identities this can be rewritten as

$$(\Delta J)_2 = \frac{\epsilon^2}{2}\int_0^1 \eta_z^2 dz + \frac{\epsilon^2}{2}\left\{\eta^2|_{z=0} + \eta^2|_{z=1}\right)\sin a\,(A\sin(2b+a-2\alpha) - \mathscr{F}\sin(2b+a-\beta))\Big\}.$$

Thus if $(A\sin(2b+a-2\alpha) - \mathscr{F}\sin(2b+a-\beta))\sin a \geqslant 0$ then $(\Delta J)_2 \geqslant 0$ for all η and the solution is stable. Otherwise it is possible to find η such that $(\Delta J)_2 < 0$ and the solution is unstable. Further manipulation of this condition can be used to show that

$$\text{Case 2 solutions are stable iff} \qquad \frac{\sin a\cos(2b+a)}{\mathscr{F}\sin\beta - A\sin 2\alpha} \geqslant 0. \tag{4.13}$$

Furthermore the condition (4.7) implies that $\cos(a+2b)$ and $(\mathscr{F}\sin\beta - A\sin 2\alpha)$ necessarily change sign at the same points (provided $\sin(\beta - 2\alpha) \neq 0$). Thus case 2 solutions change from stable to unstable, and vice-versa, only where $\sin a$ passes through a zero.

We now restrict our investigation to the solution of (4.11), for 2(i), for which $a \in (0, \pi/2)$ at $\mathscr{F} = 0$ and to the solution of (4.12), for 2(ii), for which $a \in (-\pi/2, 0)$ at $\mathscr{F} = 0$ (since these solutions are stable and global energy minimisers at $\mathscr{F} = 0$; see §3). We shall only consider loss of stability occurring as a passes through zero (this corresponds to the most likely physical scenario given the sizes of the parameters A and $(\hat{e}_1 - \hat{e}_3)$). Substituting $a = 0$ into (4.11) and (4.12) shows that stability changes at the critical values $\mathscr{F} = \mathscr{F}_{crit\pm}$ given by

$$\frac{\mathscr{F}_{crit\pm}}{A} = \frac{\cos(2\alpha-\beta) \pm [\cos^2(2\alpha-\beta) + (\hat{e}_1 - \hat{e}_3)^2\sin^2\beta - 1]^{1/2}}{1 - (\hat{e}_1 - \hat{e}_3)^2\sin^2\beta}. \tag{4.14}$$

These switching points are also points beyond which case 1 solutions cease to exist, and thus correspond to the bifurcation of a case 1 solution to a case 2 solution. Furthermore,

solution 2(i) changes stability at points

$$\mathscr{F} = \mathscr{F}_{crit\pm} \quad \text{where} \quad \frac{\mathscr{F}_{crit\pm}(\hat{e}_1 - \hat{e}_3)\sin\beta}{A} > 0, \tag{4.15}$$

while solution 2(ii) changes stability at points

$$\mathscr{F} = \mathscr{F}_{crit\pm} \quad \text{where} \quad \frac{\mathscr{F}_{crit\pm}(\hat{e}_1 - \hat{e}_3)\sin\beta}{A} < 0. \tag{4.16}$$

Note that 2(i) and 2(ii) lose stability for opposite signs of $\mathscr{F}$. Thus for a system to exhibit bistable switching under gradual changes in $\mathscr{F}$ it is a requirement that $\mathscr{F}_{crit+}$ and $\mathscr{F}_{crit-}$ have opposite signs. In other words bistable switching, by gradual changes in $\mathscr{F}$, from 2(i) to 2(ii) and vice-versa is possible if

$$(\hat{e}_1 - \hat{e}_3)^2 \sin^2\beta > 1. \tag{4.17}$$

If this condition is not satisfied but

$$\cos^2(2\alpha - \beta) + (\hat{e}_1 - \hat{e}_3)^2 \sin^2\beta - 1 > 0 \tag{4.18}$$

then switching, by gradual changes in $\mathscr{F}$, is possible in one direction only.

5 Time-dependent solutions: Switching

The preceding analysis has shown the existence of multiple steady states for our simple model, and indicated where switching might be possible in practice. However, it cannot tell us about how switching between the states might occur dynamically, by application of an electric field. To study this we consider the time-dependent equations (2.15) and (2.16). Due to their nonlinear character we investigate them numerically.

5.1 Time-dependent numerical simulations

The governing equation and boundary conditions in the presence of a constant applied electric field $\boldsymbol{E} = E(\sin\beta, 0, \cos\beta)$ are:

$$\theta_t = \theta_{zz} - \frac{\mathscr{F}^2}{\Upsilon}\sin(2\theta - 2\beta) \quad 0 < z < 1, \tag{5.1}$$

$$\pm v\theta_t = \theta_z - \frac{A}{2}\sin(2\theta - 2\alpha) + \frac{\mathscr{F}}{2}\left[\sin(2\theta - \beta) + (\hat{e}_1 - \hat{e}_3)\sin\beta\right] \quad \text{on } z = 0,\ 1. \tag{5.2}$$

An initial condition must also be prescribed, which we take to be the steady state that we are trying to switch out of, θ_1 or θ_2.

From a practical point of view, several things are desirable.

(1) Switching must be quickly achievable for visual display applications.

(2) Switching at moderate electric field strengths is needed (economy).

(3) Two-way switching is needed. Since $\mathscr{F}^2/\mathscr{D} = \Upsilon$ is constant for a given NLC (2.8), two-way switching must be possible within this constraint.

There will in general be some competition between these requirements.

5.2 Switching with $\beta = 0$

We have dimensionless parameters $\mathscr{F}$, $\mathscr{D}$ (or Υ), A, ν in our problem, together with the anchoring orientation angle α. Not surprisingly, whether or not switching occurs depends on the values of all these parameters.

Rather than explore a five-dimensional parameter space, we take fix the value of the surface anchoring strength A, the preferred anchoring angle α (taken to be $\alpha = \pi/3$ throughout the following), and the value of ν, and determine the curves in $(\mathscr{F}, \Upsilon)$-parameter space (or $(\mathscr{F}, \mathscr{D})$-parameter space, where this proves more convenient) that separate regions where switching occurs from regions where it does not. We denote the region where $\boldsymbol{n}_1$-to-$\boldsymbol{n}_2$ switching occurs by S_{12} (bounded by the curve Γ_{12}), and the region where $\boldsymbol{n}_2$-to-$\boldsymbol{n}_1$ switching occurs by S_{21} (bounded by Γ_{21}).

To determine these regions, we solve (5.1) and (5.2), starting from one of the two stable configurations. We apply a constant electric field (constant $\mathscr{D} = \mathscr{D}_0$ and $\mathscr{F} = \mathscr{F}_0$) for a fixed length of time (sufficiently long that the director field approaches equilibrium under this constant applied field), then decrease the field linearly to zero ($|\mathscr{F}|$ decreasing linearly in t, $|\mathscr{D}|$ decreasing quadratically in t).[3] The computation is then continued until the new zero-field equilibrium is reached. In all such computations the total number of timesteps taken is 10^6, with a timestep of $dt = 10^{-4}$. The constant field is applied for 2.5×10^5 timesteps, then decreased linearly over 5×10^4 timesteps. If an $\boldsymbol{n}_1$-to-$\boldsymbol{n}_2$ switch occurs in the simulation then the point $(\mathscr{F}_0, \Upsilon_0)$ (or $(\mathscr{F}_0, \mathscr{D}_0)$) is deemed to lie in S_{12}, and similarly for S_{21}.

Numerically we find that, for $\beta = 0$, Γ_{12} and Γ_{21} are exact reflections of each other in the $\mathscr{F}$-axis (Figures 5–8). This is a consequence of the scaling invariance (4.4), which sends 2(i) to 2(ii), where $a \mapsto -a$, and vice-versa.

Typical switching behaviour is shown in Figures 11 and 12.

5.2.1 *Dependence on A*

The shapes of the 'switching curves' Γ_{12} and Γ_{21} in $(\mathscr{F}, \Upsilon)$-space depend strongly on the value of the dimensionless anchoring strength A.

Curves for $A = 1.0$ and $A = 3.0$ (with $\nu = 1.0$ in each case) are shown in Figures 5 and 6. For $A = 1$, within the region $S_{12} \cap S_{21}$, both types of switching can occur. Since Υ is a material parameter, and therefore constant for any given device, two-way switching is only possible within this intersection region.

As A increases however, the region $S_{12} \cap S_{21}$ disappears, as illustrated in Figure 6. If the vertical asymptote $\mathscr{F} = \mathscr{F}_c$ to Γ_{12} and Γ_{21} is plotted as a function of A, as is

[3] It was felt that more reliable numerical results would be obtained by keeping the applied field continuous in time, hence a "ramped" profile was chosen for the electric field. It is more common for the field to be switched off instantaneously.

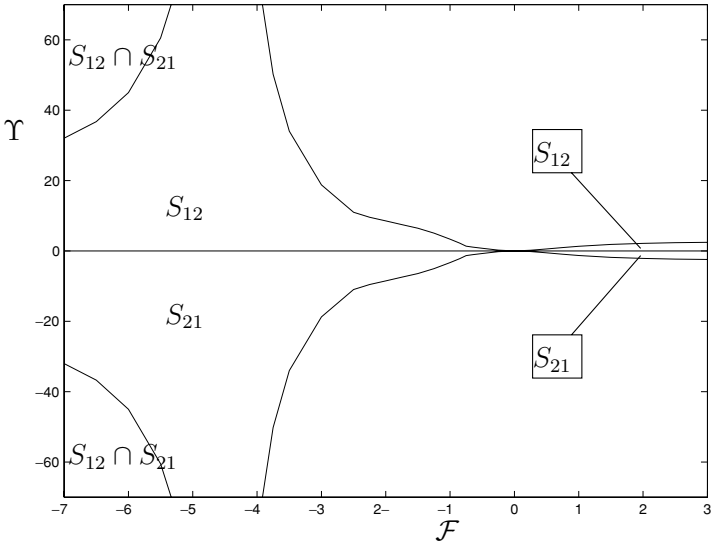

FIGURE 5. The curves Γ_{12} and Γ_{21} in $(\mathscr{F}, \Upsilon)$-parameter space, bounding the switching regions S_{12} and S_{21}, for $A = 1.0$ and $v = 1.0$. The vertical asymptote to the curves lies at $\mathscr{F} = \mathscr{F}_c$.

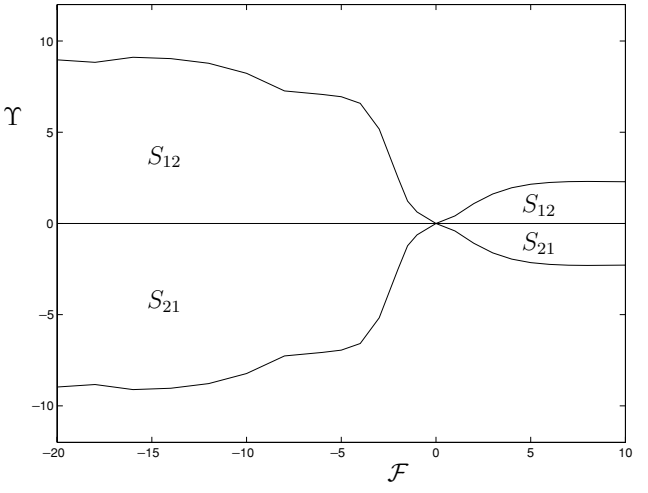

FIGURE 6. The curves Γ_{12} and Γ_{21} bounding the switching regions S_{12} and S_{21}, for $A = 3.0$ and $v = 1.0$. The asymptote $\mathscr{F} = \mathscr{F}_c$ no longer exists, and the two switching regions are disjoint, S_{12} being confined to $\Upsilon > 0$ and S_{21} to $\Upsilon < 0$. Since Υ is a material constant, it may be seen that a bistable switching device is no longer possible.

done in Figure 10 below for several values of v, it is seen that $\mathscr{F}_c \to -\infty$ for some finite value of A, $A = A_* \approx 1.21$. If $A > A_*$ then $\boldsymbol{n}_1$-to-$\boldsymbol{n}_2$ switching is possible *only* for $\Upsilon > 0$, and $\boldsymbol{n}_2$-to-$\boldsymbol{n}_1$ switching is possible *only* for $\Upsilon < 0$. Thus, since the sign of Υ cannot change for a given NLC device (it is the same as the sign of ε_a), it follows that, for $A > A_*$, a switchable bistable device of the kind proposed is not possible. If

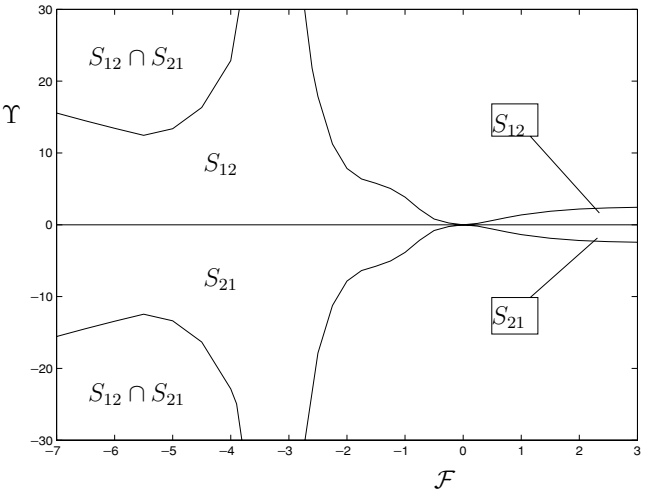

FIGURE 7. The curves Γ_{12} and Γ_{21} in $(\mathcal{F}, \Upsilon)$-space, for $A = 1.0$, $v = 0.1$.

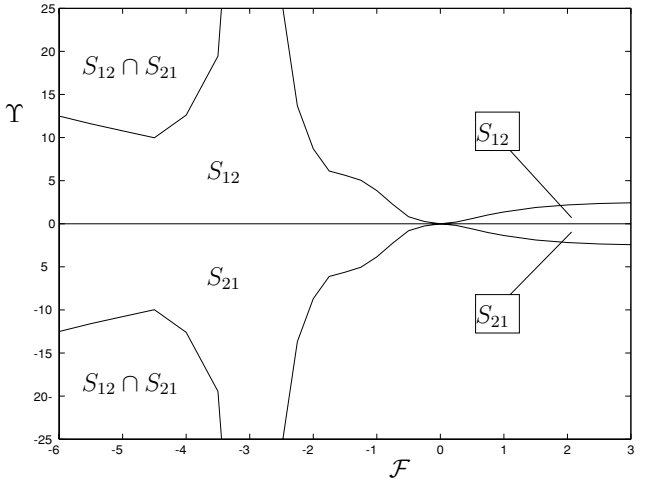

FIGURE 8. The curves Γ_{12} and Γ_{21} in $(\mathcal{F}, \Upsilon)$-space, for $A = 1.0$, $v = 0.01$.

$\Upsilon > 0$ for our device then we can only switch from solution $\boldsymbol{n}_1$ to solution $\boldsymbol{n}_2$; while if $\Upsilon < 0$ we can only switch from solution $\boldsymbol{n}_2$ to solution $\boldsymbol{n}_1$. Two-way switching is never possible.

5.2.2 *Dependence on v*

Switching behaviour is not strongly dependent on the value of v. With $A = 1.0$, the curves Γ_{12} and Γ_{21} for $v = 0.1$, 0.01, 0.001 are shown in Figures 7, 8 and 9. We observe that the region in which both types of switching are possible increases a little in size as v decreases. Apart from this feature, the curves are very little changed.

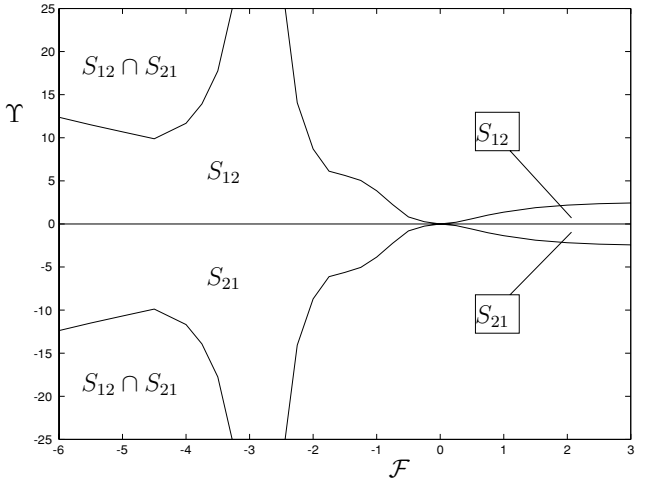

FIGURE 9. The curves Γ_{12} and Γ_{21} in $(\mathcal{F}, \Upsilon)$-space, for $A = 1.0$, $v = 0.001$.

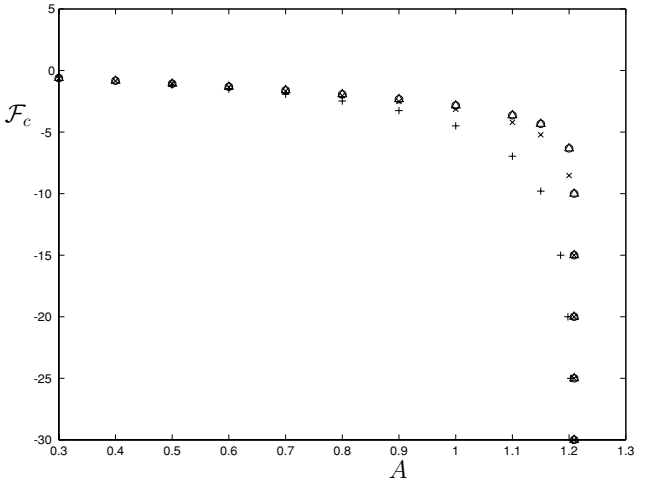

FIGURE 10. The plot of $\mathcal{F}_c$ as a function of A, for v-values $v = 1.0$ (+), $v = 0.1$ (×), $v = 0.01$ (○), $v = 0.001$ △.

The dependence of the switching curves on A also shows the same features for all values of v studied. Figure 10 plots the value of $\mathcal{F}_c$ (the vertical asymptote to Γ_{12} and Γ_{21}) as a function of A for $v = 1.0, 0.1, 0.01, 0.001$. Clearly all the curves have the same qualitative behaviour, suggesting that, independently of the value of v, there is a limiting value A_* beyond which such a bistable device will not work.

While values of the parameter v are hard to estimate, it is probable (see earlier discussions [7,14], for example) that v will be small in our problem, so that the results for $v = 10^{-3}$ are probably most relevant.

Since Υ is fixed for a given device, and since the switching curves are exactly symmetrical about the line $\Upsilon = 0$, we lose no generality by restricting attention to devices for which

$\Upsilon > 0$, as the $\Upsilon < 0$ results may be inferred from this case. We assume $\Upsilon > 0$ for the remainder of §5.2 (hence also that $\mathscr{D} \geqslant 0$).

5.2.3 *How does switching occur in practice?*

In the studies of flexoelectric-driven switching of bistable devices reported [7, 9], it was found that the electric field (and therefore $\mathscr{F}$) must be of one sign for the switch from state $\boldsymbol{n}_1$ to state $\boldsymbol{n}_2$, and of the other sign to obtain the state $\boldsymbol{n}_2$ to state $\boldsymbol{n}_1$ switch. This is not so for our hypothetical device. If we consider a particular device, so that Υ is fixed and only $\mathscr{F}$ may vary, then on the corresponding 'switching diagram' in $(\mathscr{F}, \Upsilon)$-space, all possible observed behaviour for the system in question lies on a straight line $\Upsilon = \Upsilon_0$. Figures 5, 7, 8 and 9 show the $A = 1.0$ switching diagrams for various v-values. Clearly, no line $\Upsilon = \Upsilon_0$ passes through part of S_{12} in $\mathscr{F} > 0$, and through part of S_{21} in $\mathscr{F} < 0$, and so the switching for both $\boldsymbol{n}_1$-to-$\boldsymbol{n}_2$ and $\boldsymbol{n}_2$-to-$\boldsymbol{n}_1$ must occur via an electric field such that $\mathscr{F} < 0$.

There are obviously very many possible choices of parameters that will lead to switching; however, broadly speaking, one would like to achieve switching at moderate values of the electric field, with a material for which the flexoelectric coefficient $(\tilde{e}_1 + \tilde{e}_3)$ is not too large, since for most known NLCs this parameter is rather small, of the order of 10^{-11} C m^{-1}.

Below we outline a typical two-way switching scenario. The time step is again set to be 0.0001 dimensionless time units, giving the total time of the computations as

$$\tilde{t} = 0.0001 \times N \times \frac{\tilde{\mu}\tilde{h}^2}{\tilde{K}},$$

where N is the total number of timesteps taken. Our (somewhat arbitrary) strategy is to apply a constant electric field for 0.25 times the total length of the computation, and then let the field decay over 0.05 times the total computation time. The total number of timesteps N is then reduced to give (roughly – to the nearest 5,000) the lowest value at which full switching occurs. This is the only sense in which we attempt to optimise switching times. However, we first set the values of $\mathscr{F}$ and Υ, choosing values with as small an applied field as is commensurate with switching, based on the switching diagrams obtained above. We also tried to ensure that the required flexoelectricity parameter is as small as possible, to ensure that the results will be achievable with known nematics. Therefore, the switching times reported will almost certainly not be optimal. The parameters v and A are set to $v = 0.001$, $A = 1$.

Consider first a $\boldsymbol{n}_2$-to-$\boldsymbol{n}_1$ switching scenario (the most difficult to attain, under the assumption $\varepsilon_a > 0$). The applied field must be such that the corresponding $(\mathscr{F}, \Upsilon)$-values lie in S_{21}. For $A = 1.0$, $v = 0.001$, values $\mathscr{F} = -4.5$, $\Upsilon = 10.0$ (see Figure 9) are sufficient. The corresponding switching is shown in Figure 11, which shows the director field within the sample (z is the vertical coordinate) at regular intervals during the switching process. The heads are retained on the arrows in this and the following figure simply to make the switching process easier to follow: we emphasise that the states $\pm\boldsymbol{n}$ are equivalent.

Given $\tilde{\varepsilon}_0 = 8.854 \times 10^{-12}$ C^{2}N^{-1}m^{-2}, taking $\tilde{K} = 8 \times 10^{-12}$ N (a typical value for common nematics), and $\varepsilon_a = 10$, the relation $\Upsilon = 10$ gives (see (2.8)) $(\tilde{e}_1 + \tilde{e}_3) = 5.951 \times 10^{-11}$ C m^{-1}

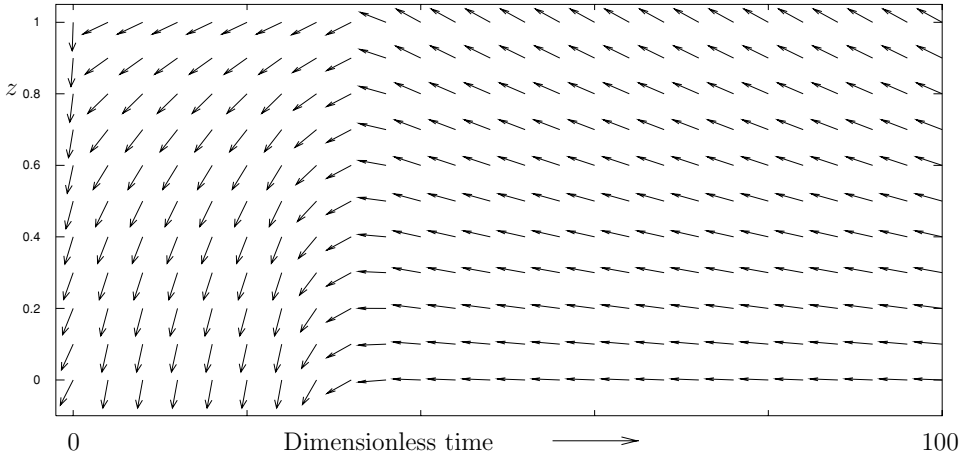

FIGURE 11. Switching between director fields $\boldsymbol{n}_2$ and $\boldsymbol{n}_1$, for $A = 1.0$, $v = 0.001$, $\alpha = \pi/3$, $\mathscr{F} = -4.5$, $\Upsilon = 10.0$. A constant electric field is applied for 25 dimensionless time units, and then decreased to zero over a further 5 time units.

as the required flexoelectricity parameter to obtain this scenario (a value commensurate with those for known nematics [2]).

To find the corresponding electric field, we must also fix the sample thickness. Taking $\tilde{h} = 0.5\,\mu$m, the required field is found (from (2.7)) to be $\tilde{E} = -1.210\,\text{V}\ \mu\text{m}^{-1}$, and the required surface energy parameter consistent with $A = 1.0$ is deduced (from (2.10)) to be $\tilde{A} = 1.6 \times 10^{-5}\,\text{N m}^{-1}$, a value which, though small, is attainable with known nematics and surfaces [1,3,11,18,22,23,26,27,34,36–38]. If one allows a thicker sample, say $\tilde{h} = 5\mu$m (a value more realistic, given the limitations of current technology) then the required electric field decreases to $\tilde{E} = -0.121\,\text{V}\ \mu\text{m}^{-1}$, while the surface energy necessary for $A = 1$ decreases to $\tilde{A} = 1.6 \times 10^{-6}\,\text{N m}^{-1}$, which is really very small.

The total computation covers 1,000,000 time steps (if one further reduces the number of steps with our chosen strategy switching does not occur, as, presumably, the field has not been applied for sufficiently long). However, switching is effectively complete shortly after removal of the field, after approximately 400,000 time steps, giving a dimensional switching time of

$$\tilde{T}_s = 0.0001 \times 400,000 \times \frac{\tilde{\mu}\tilde{h}^2}{\tilde{K}} \approx 0.125\,\text{s},$$

if $\tilde{\mu} = 0.1\,\text{N s m}^{-2}$.

To reverse the switch, a lower field will suffice, as we may move along the line $\Upsilon = 10$ out of the region S_{21}, provided we stay within S_{12} in Figure 9. Thus, the value $\mathscr{F} = -2.1$ is enough to obtain $\boldsymbol{n}_1$-to-$\boldsymbol{n}_2$ switching (Figure 12), corresponding to an electric field of $-0.565\,\text{V}\ \mu\text{m}^{-1}$. Here, we managed to reduce the computation time to 85,000 timesteps and still obtain the switching, but full switching then requires the full computation time, giving

$$\tilde{T}_s \approx 0.027\,\text{s}.$$

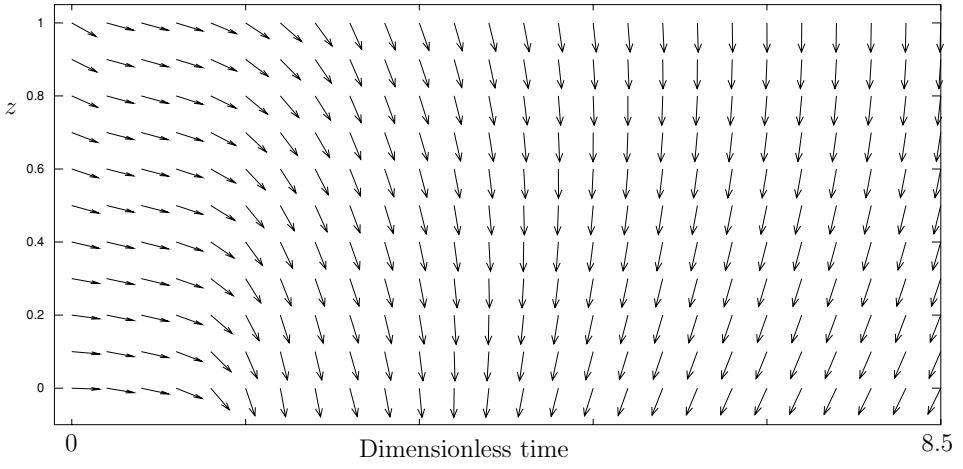

FIGURE 12. Switching between director fields $\boldsymbol{n}_1$ and $\boldsymbol{n}_2$, for $A = 1.0$, $\nu = 0.001$, $\alpha = \pi/3$, $\mathscr{F} = -2.1$, $\Upsilon = 10.0$. A constant field is applied for 2.125 time units, and then decreased to zero over a further 0.425 time units.

Again, if the sample thickness is increased by a factor of 10 then the required electric field decreases by this factor, as does the necessary dimensional surface energy at the bounding walls of the cell.

Obviously, there are very many different switching scenarios. However, there are some general features of any successful device that may be pointed out.

- The material parameter Υ cannot be too small if two-way switching is to occur. In Figures 8 and 9, for example, it can be seen that if $\Upsilon \lessapprox 10$, no $\boldsymbol{n}_2$-to-$\boldsymbol{n}_1$ switching would be possible. Thus, materials with larger values of $(\tilde{e}_1 + \tilde{e}_3)$, or smaller values of ε_a, are desirable.
- As commented earlier, with $\Upsilon = \Upsilon_0 > 0$ fixed, and sufficiently large that we have two-way switching, the switching (*both* ways) always occurs for $\mathscr{F} < 0$ (so at negative electric field $\tilde{E}$ if $(\tilde{e}_1 + \tilde{e}_3) > 0$, as is usually the case, or possibly for a positive field if $(\tilde{e}_1 + \tilde{e}_3) < 0$).
- Switching at low electric fields is desirable on energy consumption grounds. Thus, given Υ, the value of $\mathscr{F}$ at which bistable switching occurs should be as low as possible. Larger values of Υ also aid this.
- As is clear from Figures 5, 6 and 10, the dimensionless anchoring strength A cannot be too large if a switchable bistable device is to exist. From (2.10) this requires that the dimensional surface energy parameter $\tilde{A}$ and the sample thickness $\tilde{h}$ be not too large, and that the elasticity parameter $\tilde{K}$ be not too small. However, smallness of $\tilde{h}$ has implications for engineering feasibility, and smallness of $\tilde{A}$ depends on finding suitable nematic/surface pairs. Moreover, smallness of $\tilde{h}$ and largeness of $\tilde{K}$ are in conflict with the requirement for switching at low fields.
- Finally, for a usable device, the time taken to switch between the two stable states should not be too long. Although we gave approximate switching times in the above examples, we have not yet investigated this factor in any detail, or tried to optimise it.

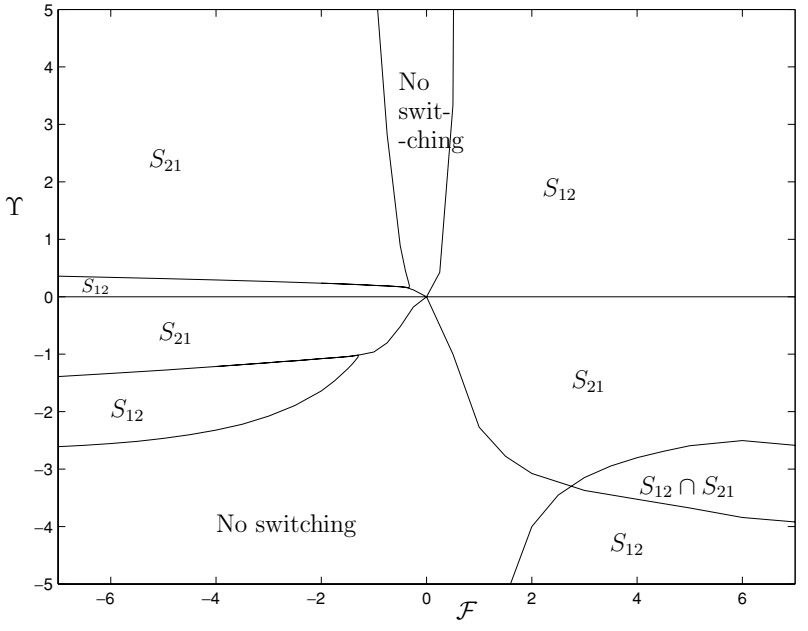

FIGURE 13. The curves Γ_{12} and Γ_{21} bounding the switching regions S_{12} and S_{21}, for $A = 1.0$, $v = 0.001$, in $(\mathcal{F}, \Upsilon)$-space.

5.3 Switching with $\beta \neq 0$

We conclude by briefly investigating the switching characteristics for a specific instance in which an electric field $\tilde{\boldsymbol{E}} = \tilde{E}(\sin\beta \boldsymbol{e}_x + \cos\beta \boldsymbol{e}_z)$ is applied in a direction that is not perpendicular to the sample. While presumably more difficult to engineer, such a device has the advantage that it can operate with smaller flexoelectric coefficient $(\tilde{e}_1 + \tilde{e}_3)$, and at smaller electric fields.

We take $\beta = \pi/4$ as in the steady-state bifurcation analysis of §4, and also specify the normalised flexoelectric coefficients (which now appear in the equations (5.1), (5.2)): $\hat{e}_1 = 0.75$, and $\hat{e}_3 = 0.25$, consistent with $(\hat{e}_1 - \hat{e}_3) = 0.5$ in the analysis of §4. These values are a little arbitrary, as the individual flexoelectric coefficients are rarely determined (more usually their sum is determined). However, the studies by Cheung [5] and Murthy *et al.* [20] suggest that the above choices are probably reasonable. The surface parameter $A = 1.0$ and anchoring angle $\alpha = \pi/3$, as usual.

The switching regions S_{12} and S_{21} are shown in Figure 13. The switching diagram is no longer symmetric about the $\mathcal{F}$-axis, and the switching characteristics depend on whether ε_a (and hence Υ, or $\mathcal{D}$) is positive or negative.

Consider first $\Upsilon > 0$. It can be seen from Figure 13 that, while $\boldsymbol{n}_1$-to-$\boldsymbol{n}_2$ switching is possible for any positive value of Υ (for some $\mathcal{F} > 0$), only values of Υ larger than about 0.2 will allow $\boldsymbol{n}_2$-to-$\boldsymbol{n}_1$ switching (this is much less restrictive than the $\beta = 0$ case considered above). This is consistent with the analysis of §4, where (within the limitations of the steady-state analysis) it was deduced that a switchable device required $\Upsilon > 0.305$ (approximately). With $\Upsilon = 0.25$, for example, $\boldsymbol{n}_2$-to-$\boldsymbol{n}_1$ switching with a negative field

$\mathscr{F} < 0$ is possible; and in this case the values used earlier: $\tilde{\varepsilon}_0 = 8.854 \times 10^{-12}$ $C^2N^{-1}m^{-2}$, $\tilde{K} = 8 \times 10^{-12}$ N, and $\varepsilon_a = 10$, give $(\tilde{e}_1 + \tilde{e}_3) = 9.41 \times 10^{-12}$ C m^{-1} as the required flexoelectricity parameter.[4]

Taking $\mathscr{F} = -0.36$ is sufficient to obtain $\boldsymbol{n}_2$-to-$\boldsymbol{n}_1$ switching, and the corresponding electric field (again with a sample thickness $\tilde{h} = 0.5\,\mu$m) is found to be $\tilde{E} = -0.61$ V μm^{-1}, from which the required surface energy parameter consistent with $A = 1.0$ is again deduced (from (2.10)) to be $\tilde{A} = 1.6 \times 10^{-5}$ N m^{-1}. As before, increasing $\tilde{h}$ leads to corresponding decreases in the required electric field strength $\tilde{E}$ and dimensional surface energy parameter $\tilde{A}$.

For the reverse $\boldsymbol{n}_1$-to-$\boldsymbol{n}_2$ switching, an even smaller electric field will suffice. The value $\mathscr{F} = 0.25$ lies within S_{12} in Figure 13 (with $\Upsilon = 0.25$), and corresponds to the electric field $\tilde{E} = 0.43$ V μm^{-1}.

For $\varepsilon_a < 0$ ($\Upsilon < 0$, $\mathscr{D} < 0$), switching can again be obtained, though not for quite such a large parameter range as when $\varepsilon_a > 0$. Two-way switching may be obtained for moderate values of $\mathscr{F}$ in roughly the ranges $-4.0 \lessapprox \Upsilon \lessapprox -1.0$. So, for example, $\Upsilon = -1.05$ will do, corresponding to flexoelectric coefficients $(\tilde{e}_1 + \tilde{e}_3) = 1.928 \times 10^{-11}$C m^{-1}. $\boldsymbol{n}_1$-to-$\boldsymbol{n}_2$ switching can then be obtained with $\mathscr{F} = -1.55$, corresponding to an electric field $\tilde{E} = -1.29$ V μm^{-1}. $\boldsymbol{n}_2$-to-$\boldsymbol{n}_1$ switching can be obtained with $\mathscr{F} = 0.6$, corresponding to an electric field $\tilde{E} = 0.498$ V μm^{-1}.

6 Conclusions

We have proposed a simple, idealised, bistable nematic device, which relies on the different anchoring properties of the two bounding surfaces at $\tilde{z} = 0$ and $\tilde{z} = \tilde{h}$. Switching between the two stable states operates by means of an electric field, applied at some angle β (which may be zero) relative to the z-axis.

As stated in § 2, certain assumptions were made in order to obtain a sufficiently simple model to analyse. Most questionable of these is probably our assumption that the electric field is uniform within the sample. As we point out in § 2, there will in reality be coupling between the director field and the electric field, and it is not clear whether, if included, such coupling would enhance or hinder the observed switching behaviour. This is an important point, which requires further investigation.

A dimensionless material parameter, $\Upsilon = 2(\tilde{e}_1 + \tilde{e}_3)^2/(\tilde{K}\varepsilon_0\varepsilon_a)$ is identified, which may be used to characterise whether or not switching occurs in different situations. A time-independent bifurcation analysis was first carried out to investigate switching. In the asymptotic limit $\Upsilon \to 0$, in which the flexoelectric effects dominates the dielectric effect, bistable switching was found to be possible if

$$(\hat{e}_1 - \hat{e}_3)^2 \sin^2 \beta > 1.$$

Thus, crucially in this limit, it is a requirement that the electric field is applied at an angle to the sample. Within the limitations of the more general (numerical) time-independent bifurcation investigation, this finding was also confirmed. However this does not exclude

[4] Note that this is considerably smaller than the values required for bistable switching in the case $\beta = 0$.

the possibility of a bistable device at $\beta = 0$, since field-driven switching is a time-dependent process, and dynamic effects are not captured by the bifurcation analysis.

Thus, a numerical study of the time-dependent problem was also undertaken. A common 'switching protocol' was used for all simulations: the electric field was applied at a constant level for a fixed time, before being decreased linearly to zero, again over a fixed time interval. In the case $\beta = 0$, which is the case in most applications, a parameter study was carried out for several different values of the dimensionless anchoring strength A. The regions of $(\mathscr{F}, \Upsilon)$-space in which switching is possible under the adopted protocol were mapped out, and from these parameter-space plots it is apparent that A must not be too large if the device is to be operable. Numerically, for $\beta = 0$, we required $A < A_* \approx 1.21$. For $A < A_*$ the switching mechanism was investigated, and sample switching scenarios were presented.

A brief investigation into time-dependent switching when the electric field is not perpendicular to the plates was also carried out in § 5.3.

In our time-dependent simulations we concentrated mainly on achieving the switching at the smallest possible fields, and at low values of the flexoelectric coefficient $(\tilde{e}_1 + \tilde{e}_3)$. Thus, we have not yet investigated in detail how switching time may be minimised. Suffice it to say that the simulations we present are not optimised in this regard; we could certainly apply (for example) a higher electric field for a shorter time and still obtain switching.

We acknowledge that certain parameter values required to obtain the two-way switching may be on the edge of, if not somewhat beyond, current liquid crystal technologies. To have the dimensionless surface energy $A \approx 1$ (as is needed) we require either a value of the anchoring strength $\tilde{A}$ that is at the bottom end of that found for real NLC-substrate systems (systems with similarly low anchoring strengths are reported elsewhere [1, 3, 11, 18, 22, 23, 26, 27, 34, 36–38]), or a cell width $\tilde{h}$ that is rather smaller than can be reliably engineered at present. However, liquid crystal research continues to advance rapidly (for example many recent strides have been made in surface treatments that can generate specified anchoring properties [6, 13, 25, 30, 31], and the precision with which cells can be manufactured is constantly improving). Moreover, we have investigated only one very simple case, in which the anchoring at the opposing (planar) surfaces of the device is $\pi/2$ out of phase, leading to a model in which the director field depends only on the coordinate perpendicular to the surfaces. Obviously, many variations on this theme, including the effect of a variable upper surface $z = h(x, y)$, are possible, and may lead to other bistable devices that do not suffer from the restrictions of ours; namely that the dimensionless anchoring strength must not be too large, and that engineering the bounding surfaces with the required properties may be a delicate matter.

Nevertheless, the fact that our idea works in principle suggests that future investigation along similar lines will be fruitful. If a device based on the principles we suggest can be engineered, it offers the potential for a simple switchable bistable device that can operate at low electric fields, and that does not require materials with very large flexoelectric polarisation.

Acknowledgements

We thank Drs Chris Newton and Tim Spiller of Hewlett-Packard laboratories (Bristol) for drawing the problem to our attention, and for very helpful discussions. LJC gratefully

acknowledges financial support from the National Grid plc in the form of a Royal Society Dorothy Hodgkin Research Fellowship. Two anonymous referees also provided many helpful comments on earlier versions of this manuscript.

References

[1] Barberi, R., Dozov, I., Giocondo, M., Iovane, M., Martinot-Lagarde, Ph., Stoenescu, D., Tonchev, S. & Tsonev, L.V. (n.d.) Azimuthal anchoring of nematic on undulated substrate: Elasticity versus memory. *http://www.nemoptic.com/binem/publications.htm*

[2] Blinov, L.M., Kolovsky, M., Nagata, T., Ozaki, M. & Yoshino, K. (1999) Influence of guest conformation (rod- or banana-like photo-isomers) on flexoelectric coefficients in nematic liquid crystals. *Jpn. J. Appl. Phys.* **38**, L1042–L1045.

[3] Blinov, L. M., Kabayenkov, A. Yu & Sonin, A. A. (1989) Invited Lecture: Experimental studies of the anchoring energy of nematic liquid crystals. *Liquid Crystals* **5** (2), 645–661.

[4] Brown, C. V., Bryan-Brown, G. P. & Jones, J. C. (2001) Bistable nematic liquid crystal device. U.S. Patent no. 6,249,332 (19th June).

[5] Cheung, D. L. G. (2002) Structures and properties of liquid crystals and related molecules from computer simulation. *PhD Thesis, Univ. Durham, Chemistry*. http://portellen.phycmt.dur.ac.uk/sjc/thesis_dlc/thesis.html

[6] Cui, L., Jin, W., Liu, Y., Xie, P., Zhang, R., Zhu, C. & Wang, C. (1999) A combined method based on rubbing and UV-irradiation for preparing stable alignment layers with high pretilt angles. *Mol. Crys. Liq. Cryst.* **333**, 135–144.

[7] Davidson, A. J. & Mottram, N. J. (2002) Flexoelectric switching in a bistable nematic device. *Phys. Rev. E*, **65**, 051710.

[8] De Gennes, P. G. & Prost, J. (1993) *The Physics of Liquid Crystals (2nd ed.)*. International Series of Monographs on Physics (83), Oxford Science Publications.

[9] Denniston, C. & Yeomans, J. M. (2001) Flexoelectric surface switching of bistable nematic devices. *Phys. Rev. Lett.* **87** (27), Art. no. 275505.

[10] Doedel, E. J., Champneys, A. R., Fairgrieve, T. F., Kuznetsov, Yu. A., Sandstede, B. & Wang, X. (1998) Auto 97: continuation and bifurcation software for ordinary differential equations. Available free at *ftp.cs.concordia.ca*, directory pub/doedel/auto.

[11] Dozov, I. & Martinot-Lagarde, Ph. (n.d.) New bistable nematic LCDs using a weak anchoring boundary. *http://www.nemoptic.com/binem/publications.htm*

[12] Ericksen, J. L. (1960) Anisotropic Fluids. *Arch. Rat. Mech. Anal.* **4** (3), 231–237.

[13] Hwang, J.-Y., Lee, S. H., Paek, S. K. & Seo, D.-S. (2003) Tilt angle generation for nematic liquid crystal on blended homeotropic polyimide layer containing Trifluoromethyl moieties. *Jpn. J. Appl. Phys.* **42** (1), 1713–1714.

[14] Kedney, P. J. & Leslie, F. M. (1998) Switching in a simple bistable nematic cell. *Liquid Crystals*, **24** (4), 613–618.

[15] Leslie, F. M. (1979) Theory of flow phenomena in liquid crystals. *Advances in Liquid Crystals*, **4**, 1–81.

[16] Leslie, F. M. (1968) Some constitutive equations for liquid crystals. *Arch. Ration. Mech. Anal.* **28**, 265–283.

[17] Leslie, F. M. (1966) Some constitutive equations for anisotropic fluids. *Q. J. Mech. Appl. Math.* **19**, 357 & Part 3.

[18] Mada, H. & Sato, S. (1999) Pretilt angle dependence of azimuthal anchoring energy in nematic liquid crystals. *Jpn. J. Appl. Phys.* **38**, L1118–L1120.

[19] Martinot-Lagarde, P., Durand, G., Barberi, R. & Giocondo, M. (1994) U.S. Patent no. 5,357,358 (18th October).

[20] Murthy, P. R. M., Raghunathan, V. A. & Madhusudana, N. V. (1993) Experimental determination of the flexoelectric coefficients of some nematic liquid crystals. *Liquid Crystals*, **14** (2), 483–496.

[21] Newton, C. J. P. & Spiller, T. P. (2001) A novel approach to modelling nematic liquid crystal cells. *Mol. Cryst. and Liq. Cryst.* **372**, 167–178.
[22] O'Neill, M. & Kelly, S. M. (2000) Photoinduced surface alignment for liquid crystal displays. *J. Phys. D: Appl. Phys.* **33**, R67–R84.
[23] Okubo, K., Kimura, M. & Akahane, T. (2003) Measurement of genuine azimuthal anchoring energy in consideration of liquid crystal molecular adsorption on alignment film. *Jpn. J. Appl. Phys.* **42**, 6428–6433.
[24] Rapini, A. & Papoular, M. (1969) Distorsion d'une lamelle nématique sous champ magnétique. Conditions d'ancrage aux parois. *J. Phys. Colloque. C4*, **30**, 54–56.
[25] Reznikov, Y., Petschek, R. G. & Rosenblatt, C. (1996) Magnetic field-mediated alignment of a nematic liquid crystal at a polymer surface exposed to ultraviolet light. *Appl. Phys. Lett.* **68**(16), 2201–2203.
[26] Ryschenkow, G. & Kleman, M. (1976) Surface defects and structural transitions in very low anchoring energy nematic thin films. *J. Chem. Phys.* **64** (1), 404–412.
[27] Sato, Y., Sato, K. & Uchida, T. (1992) Relationship between rubbing strength and surface anchoring of nematic liquid crystal. *Jpn. J. Appl. Phys.* **31**, L579–L581.
[28] Scalerandi, M., Pagliusi, P., Cipparrone, G. & Barbero, G. (2004) Influence of the ions on the dynamical response of a nematic cell submitted to a dc voltage. *Phys. Rev. E*, **69**, 051–708.
[29] Self, R. H., Please, C. P. & Sluckin, T. J. (2002) Deformation of nematic liquid crystals in an electric field. *Europ. J. Appl. Math.* **13**, 1–23.
[30] Seo, D.-S. (1999) Generation of high pretilt angle and surface anchoring strength in nematic liquid crystal on a rubbed polymer surface. *J. Appl. Phys.* **86** (7), 3594–3597.
[31] Seo, D.-S. (2000) Anchoring strength and high pretilt angle in NLC on rubbed organic solvent soluble polyimide surfaces with trifluoromethyl moieties. *J. Korean Phys. Society*, **36**(1), 29–33.
[32] Sikharulidze, D. (n.d.) Bistable nematic liquid crystal device. U.S. Patent Application no. 20030210375.
[33] Sikharulidze, D. (n.d.) Bistable nematic liquid crystal display device. U.S. Patent Application no. 20040144953.
[34] Slavinec, M., Crawford, G. D., Kralj, S. & Zumer, S. (1997) Determination of the nematic alignment and anchoring strength at the curved nematic-air interface. *J. Appl. Phys.* **81**(5), 2153–2156.
[35] Stewart, I. W. (2004) *The Static and Dynamic Continuum Theory of Liquid Crystals.* Taylor & Francis.
[36] Vilfan, M. & Copic, M. (2003) Azimuthal and zenithal anchoring of nematic liquid crystals. *Phys Rev. E*, **68**, 031–704.
[37] Yamaguchi, R., Yamanaka, T. & Sato, S. (2001) Liquid crystal optical rotator using weak azimuthal anchoring surface. *Jpn. J. Appl. Phys.* **40**, 6522–6525.
[38] Yokoyama, H. & van-Sprang, H. A. (1985) A novel method for determining the anchoring energy function at a nematic liquid crystal-wall interface from director distortions at high fields. *J. Appl. Phys.* **57**(10), 4520–4526.